*Mineralogical Magazine, December 2015, Vol. 79(7), pp. 1779–1789*

# Electronic and chemical structures of pyrite and arsenopyrite

Yu-Qiong Li[1], Qian He[1], Jian-Hua Chen[1,*] and Cui-Hua Zhao[2]

[1] College of Resources and Metallurgy, Guangxi University, Nanning 530004, China
[2] College of Material Science and Engineering, Guangxi University, Nanning 530004, China

[*Received 2 January 2014; Accepted 8 March 2015; Associate Editor: W. Crichton*]

**ABSTRACT**

The first-principles plane-wave pseudopotential method is used to study the electronic and chemical structures of pyrite ($FeS_2$) and arsenopyrite (FeAsS). The results indicate that an antibonding interaction occurs between Fe and As atoms in arsenopyrite. This interaction results in the Fe atom being repelled towards the S atom to stabilize antibonding orbitals, causing a larger S–Fe–S angle in arsenopyrite than in pyrite and a distortion in the arsenopyrite structure. In arsenopyrite, Fe–Fe distances are alternately long and short. The low spin density of the Fe *d* electrons supports this configuration in arsenopyrite. However, electron density calculations indicate that there is negligible electron density present between Fe atoms. This result indicates that cation-anion interactions are dominant in arsenopyrite. The pyrite Fe 3*d* orbital is split below the Fermi level, whereas the arsenopyrite Fe 3*d* orbital is not split, which can be attributed to the stronger interatomic bonding effects between Fe and S atoms in pyrite compared to arsenopyrite. It is found that the *d*-*p* orbital interactions between Fe and S atoms lead to bonding-antibonding splitting in both pyrite and arsenopyrite. However, the bonding effects between pyrite Fe and S atoms are stronger than in arsenopyrite. In arsenopyrite, the bonding interaction between the As 4*p* and Fe 3*d* orbitals is very weak, while the antibonding effect is very strong. The *p*-*p* orbital interaction is the dominant effect in As–S bonding. Frontier orbital calculations indicate that the Fermi levels of pyrite and arsenopyrite are notably close to each other, resulting in similar electrochemical activities. Orbital coefficient results show that the pyrite Fe 3*d* and S 3*p* orbitals are the active orbitals in the highest occupied molecular orbital (HOMO) and lowest unoccupied molecular orbital (LUMO), respectively. In the case of arsenopyrite, Fe 3*d* orbitals are very active in both the HOMO and LUMO. Moreover, the activity of the As 4*p* in the HOMO is greater than S 3*p*, whereas the opposite situation occurs in the LUMO. Based on these results, As atoms could be one of the active sites for the oxidation of arsenopyrite. In addition, separation of arsenopyrite and pyrite could be achieved by utilizing the difference in chemical reactivities of iron in the two minerals.

**Keywords:** pyrite, arsenopyrite, density functional theory, electronic structures, frontier orbitals.

## Introduction

Pyrite ($FeS_2$) and arsenopyrite (FeAsS) are two major sulfur minerals, often found together in Nature. In mineral processing, the separation of these two minerals is difficult. They show many similar properties, such as crystal structure, oxidation behaviour, flotation behaviour and so on.

As–S separation is often difficult to achieve. Allison *et al*. (1972) found that the rest potentials of pyrite and arsenopyrite were the same in potassium ethyl xanthate at pH 7 and the same product (dixanthogen) was formed after xanthate interacted with the two minerals' surfaces. In addition, the natural oxidation rates of the minerals are very similar in buffered solution. This behaviour makes separation of the minerals difficult. Although they have very similar properties, there are still some differences between them. Fernandez *et al*. (1996) found that the oxidation rate of arsenopyrite could be accelerated significantly by the presence of sodium carbonate and sodium sulfate. We think that the difference between the minerals is affected mainly by their electronic

* E-mail: jhchen1971@sina.com
DOI: 10.1180/minmag.2015.079.7.05

and chemical structures and that these should be studied further.

The crystal structures of pyrite and arsenopyrite have been studied extensively (Huggins, 1922; Ramsdell, 1925; Buerger, 1936; Morimoto and Clark, 1961; Bayliss, 1977, 1989; Fuess *et al.*, 1987; Prince *et al.*, 2005; Bindi *et al.*, 2012). Earlier workers suggested that an excess of sulfur tends to lower the symmetry of arsenopyrite to triclinic, and a large amount of arsenic precludes monoclinic symmetry. It is concluded that most natural arsenopyrites are sulfur-rich. However, a study by Bindi *et al.* (2012) showed that stoichiometric arsenopyrite is monoclinic, space group $P2_1/c$. Pyrite is diamagnetic with $Fe^{2+}$ in low-spin configuration ($t_{2g}^{6}\ e_g^{0}$). This configuration supports the cubic symmetry of pyrite. In addition to Fe ions, dianion groups ($S_2^{2-}$, $AsS^{3-}$) occur in the crystal structures of pyrite and arsenopyrite. Eyert *et al.* (1998) confirmed that the chemical stability results mainly from Fe–S bonding. Goodenough (1972) found that structure-determining interactions were cation-anion interactions and not cation-cation interactions. However, Tossell *et al.* (1981) suggested that, to fully understand the structural and spectroscopic properties of the disulfides and related compounds, the S–S structural units must be considered in addition to the metal–S structural units.

Electronic interactions have a significant role in the structural and chemical properties of crystals. Nickel (1968) and Hulliger and Mooser (1965) identified structural variations as a function of the interactions of *d* electrons on metals. Tossell *et al.* (1981) proposed that the systematic increase in unit-cell dimension across the series from $FeS_2$ to $ZnS_2$ could be explained by increasing occupancy of the antibonding $e_g^*$ orbitals of the metal. Finklea *et al.* (1976) found that a very small amount of electron delocalization was enough to cause the quadrupole splitting observed in the Mössbauer spectra due to the strong effects of the valence electrons on iron in pyrite. Using quantitative molecular orbital (MO) calculations, Tossell *et al.* (1981) suggested that structural preferences could be understood by considering the electron occupations of a set of molecular orbitals. The study by Eyert *et al.* (1998) also showed that the S 3*p* state at the conduction band minimum is very important for the properties of pyrite, and small deviations in the sulfur pair bond lengths resulted in drastic changes in near-gap electronic states.

The electronic structure of pyrite has been studied widely (Edelro *et al.*, 2003; Von Oertzen *et al.*, 2005*a*,*b*; Womes *et al.*, 1997; Opahle *et al.*, 2000; Eyert *et al.*, 1998). It has been suggested that arsenic could be present at the sulfur site in pyrite, resulting in the formation of $AsS^{3-}$ dianions in the lattice (Abraitis *et al.*, 2004; Blanchard *et al.*, 2007). However, there have been few studies on arsenopyrite (Corkhill *et al.*, 2011). The exact electronic structure of arsenopyrite is still insufficiently understood. Moreover, no comparison results have been published. It is believed that the crystal properties have a critical role in the processing of this mineral and just small differences in crystal properties may lead to great differences in flotation behaviour. For example, Chanturiya *et al.* (2000) found that pyrite with high contents of Cu, As and Au impurities can be floated effectively at pH 11.8–12.2, while the recovery rate of pyrite with low contents of copper and a high content of sulfur vacancies does not exceed 25% under these high-pH conditions. To understand the various differences between pyrite and arsenopyrite, it is necessary to investigate their electronic and chemical structures. The present study uses first principles quantum mechanical calculations, from which atomic-scale phenomena can be clearly observed, to obtain detailed electronic and geometric structures and frontier orbital information about pyrite and arsenopyrite. This helps to describe differences in properties between the minerals. Moreover, our results are useful to provide theoretical guidance for the separation of pyrite and arsenopyrite, one of the difficult subjects in mineral processing.

## Computational methods

Based on density functional theory, structural optimizations and electronic calculations were performed using *CASTEP, GGA-PW91* (Perdew *et al.*, 1992). Only the valence electrons (Fe $3d^6 4s^2$, S $3s^2 3p^4$ and As $4s^2 4p^3$) were considered explicitly through the use of ultrasoft pseudopotentials (Vanderbilt, 1990). A plane-wave cut-off energy of 300 eV was used, and a Monkhorst-Pack (Monkhorst and Pack, 1976; Pack and Monkhorst, 1977) k-point sampling density of 4 × 4 × 4 mesh was used for both pyrite and arsenopyrite. The convergence tolerances for the geometry optimization calculations were set to a maximum displacement of 0.002 Å, a maximum force of 0.05 eV $Å^{-1}$, a maximum energy change of $2.0 \times 10^{-5}$ eV $atom^{-1}$ and a maximum stress of 0.1 GPa. The self-consistent field (SCF) convergence tolerance was set to $2.0 \times 10^{-6}$ eV $atom^{-1}$. Frontier orbital



https://doi.org/10.1180/minmag.2015.079.7.05 Published online by Cambridge University Press

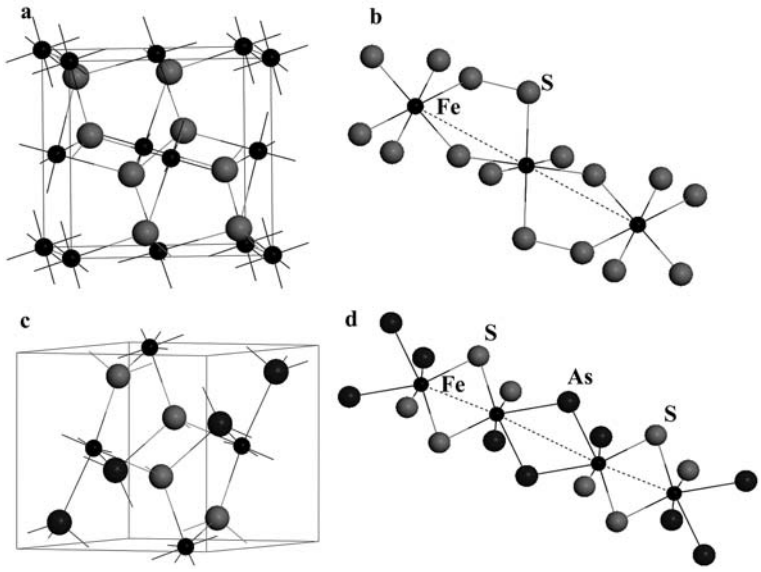


FIG. 1. (*a*) The unit cell of pyrite and (*b*) the relationship between neighbouring Fe atoms; and (*c*) the unit cell of arsenopyrite and (*d*) the relationship between neighbouring Fe atoms.

calculations were performed using DMol$^3$, a single-point energy method, the *GGA-PW91* method, DNP basis set, effective core potentials, a fine quality and an SCF convergence threshold of $1.0 \times 10^{-6}$ eV atom$^{-1}$. The spin calculation was performed during the simulation using different wave functions for different spins (Hohenberg and Kohn, 1964; Kohn and Sham, 1965; Von Barth and Hedin, 1972; Vosko *et al*., 1980; Cocula *et al*., 2003).

## Results and discussion

### *Crystal structure differences between pyrite and arsenopyrite*

Pyrite crystallizes in space group $Pa\bar{3}$. As stated previously, arsenopyrite has two possible symmetries, monoclinic and triclinic. To obtain a reasonable structure for the present calculation, we calculated and compared the monoclinic and triclinic arsenopyrite results. The results for triclinic arsenopyrite and monoclinic arsenopyrite are almost identical, including the unit-cell dimensions, interatomic distances, Fermi levels and orbital coefficients for the frontier orbitals. In addition, we also calculated the total energies of the two unit cells. The values for triclinic and monoclinic arsenopyrite were found to be similar, 5278.119 and –5278.120 eV, respectively. The recent report by Bindi *et al*. (2012) suggests that stoichiometric arsenopyrite has monoclinic symmetry with space group $P2_1/c$. Because the cell ($Fe_4As_4S_4$) used in our calculation had an ideal chemical composition, the monoclinic cell was adopted.

The unit cells of pyrite and arsenopyrite are shown in Fig. 1. The pyrite cell contains four $FeS_2$ units and the arsenopyrite unit cell four FeAsS units. The dianions in pyrite and arsenopyrite are $S_2^{2-}$ and $AsS^{3-}$, respectively. For each mineral, the cation (Fe) is octahedrally coordinated by six anions, and each of the anions is tetrahedrally coordinated by three Fe ions and one other anion. Table 1 lists the calculated crystal structural parameters of pyrite and arsenopyrite compared with results from the literature. The calculated results are consistent with the experimental values (<1% error), suggesting that the calculation method for this study is reliable. By comparing S–Fe–S angles in pyrite with those in arsenopyrite, it is found that the S–Fe–S angle is close to 90º in pyrite and obtuse in arsenopyrite, implying a greater distortion of the octahedral symmetry of Fe in arsenopyrite. This is related to the internal bonding of the crystal, discussed later.

It was confirmed by Buerger (1939) that interatomic distances in the arsenopyrite group are quite different from those of the pyrite group.



https://doi.org/10.1180/minmag.2015.079.7.05 Published online by Cambridge University Press

TABLE 1. Cell parameters and angles for pyrite and arsenopyrite.

| | Literature | | | Calculated result | | |
|---|---|---|---|---|---|---|
| | Cell parameters (Å) | β (°) | S–Fe–S (°) | Cell parameters (Å) | β (°) | S–Fe–S (°) |
| Pyrite* | $a = b = c = 5.417$ | 90.0 | 85–95 | $a = b = c = 5.386$ | 90.0 | 85.5–94.5 |
| Arsenopyrite** | $a = 5.761$, $b = 5.684$, $c = 5.767$ | 111.7 | 104.35 | $a = 5.701$, $b = 5.636$, $c = 5.720$ | 111.8 | 104.9 |

*Bayliss (1977); **Bindi *et al*. (2012).

Table 2 lists interatomic distances and Mulliken bond populations in pyrite and arsenopyrite. In pyrite, the lengths of the six Fe–S bonds (2.247 Å) are equivalent, whereas for arsenopyrite the lengths of the three Fe–As bonds and the three Fe–S bonds are different, ranging from 2.366 to 2.403 Å and 2.174 to 2.209 Å, respectively. Interatomic S–S distances in pyrite and As–S in arsenopyrite are 2.186 Å and 2.396 Å, respectively. The Fe–Fe distance in pyrite is 3.808 Å, which is much longer than in arsenopyrite (a short distance of 2.657 Å and a longer distance of 3.746 Å).

Hulliger and Mooser (1965) and Tossell *et al*. (1981) showed that two neighbouring Fe have a common corner in pyrite, while they share an edge in arsenopyrite (Fig. 1). It was noted by Goodenough (1960) that the interactions between two octahedral cations will be cation-anion-cation interactions if the two octahedra share a common corner, but may be cation-cation interactions if the two octahedra share a common edge. These configurations support the low-spin states of pyrite and arsenopyrite. In pyrite Fe has the low-spin configuration $t_{2g}^6 e_g^0$, while in arsenopyrite Fe has a high-spin $d^5$ configuration, which cannot be paired in the $t_{2g}$ orbitals. However, spin pairing can be achieved if the unpaired electron in one of the $t_{2g}$ orbitals of one atom is paired with an unpaired electron of an adjacent metal atom across the octahedral edge (Hulliger and Mooser, 1965; Nickel, 1968). Consequently, in arsenopyrite, the Fe–Fe distances are alternately long and short. A magnetic moment of zero supports the low spin configuration for the arsenopyrite structure (Hulliger and Mooser, 1965). Our calculation also yields a low spin density for the Fe *d* electrons in both pyrite and arsenopyrite.

The bond population result shows that the covalent S–S interactions in pyrite (0.22) are weaker than As–S in arsenopyrite (0.28). It is interesting that the population value of the Fe–As bond is negative, suggesting an anti-bonding interaction between Fe and As atoms. This situation will result in Fe atoms being repelled towards S atoms to stabilize antibonding orbitals. According to Goodenough (1972), these cation-anion repulsive forces may cause distortion in the arsenopyrite structure. The population value of Fe–S in pyrite (0.34) is smaller than that in arsenopyrite (0.40–0.44), suggesting that the covalent interaction in the

TABLE 2. Interatomic distances and Mulliken populations of bonds in pyrite and arsenopyrite.

| | Pyrite | | | Arsenopyrite | | | |
|---|---|---|---|---|---|---|---|
| | Fe–S | S–S | Fe–Fe | Fe–S | Fe–As | As–S | Fe–Fe |
| Calculated distance (Å) | 2.247 | 2.186 | 3.808 | 2.174–2.209 | 2.366–2.403 | 2.396 | 2.657, 3.746 |
| Population* | 0.34 | 0.22 | | 0.40–0.44 | –0.17 to –0.26 | 0.28 | – |
| Literature distance (Å)** | 2.23–2.30 | 2.14–2.17 | | 2.229–2.233 | 2.370–2.412 | 2.374 | 2.734, 3.741 |

*Higher Mulliken population values indicates stronger covalent interaction between atoms and negative values indicate anti-bonding interactions (Segall *et al*., 1996). **Pyrite literature from Bayliss (1977); monoclinic arsenopyrite literature from Bindi *et al*. (2012).



https://doi.org/10.1180/minmag.2015.079.7.05 Published online by Cambridge University Press

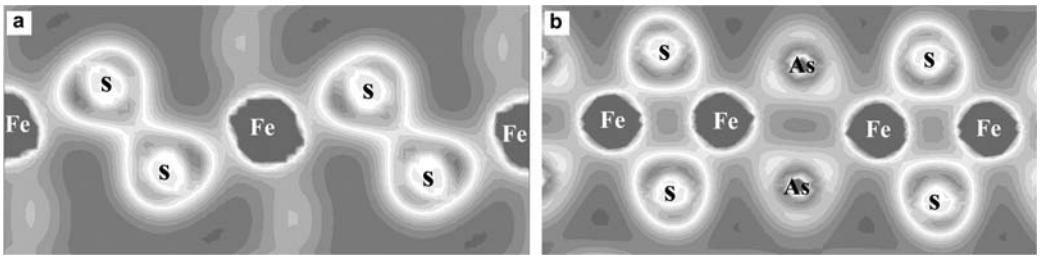


FIG. 2. Electron density maps between (*a*) S–S and Fe–S atoms in pyrite and (*b*) Fe–S and As–S in arsenopyrite. A greater degree of electron overlaps indicate a stronger covalent interaction.

former is weaker than in the latter. This apparently greater covalent interaction is clearly shown in the electron density map (Fig. 2*a*,*b*), from which it is clear that the electron density in the arsenopyrite Fe–S region is greater than that in the pyrite Fe–S region. Based on the arsenopyrite map, there is no electron density present between Fe atoms (for both short and long separations), which indicates that the cation-cation interaction is very weak even at these distances and that cation-anion interactions are dominant in arsenopyrite. This result is consistent with the view of Goodenough (1960) and Tossell *et al*. (1981) that structure-determining interactions are attributed to be cation-anion and not cation-cation interactions.

## *Electronic structures*

Electronic band structures and corresponding densities of states (DOS) of pyrite and arsenopyrite are shown in Fig. 3 (zero point energies were set at the Fermi level, $E_F$). There are DOS at the Fermi energy level for pure pyrite or arsenopyrite, which are insulating materials. This is caused by the Gaussian broadening used in the DOS calculation.

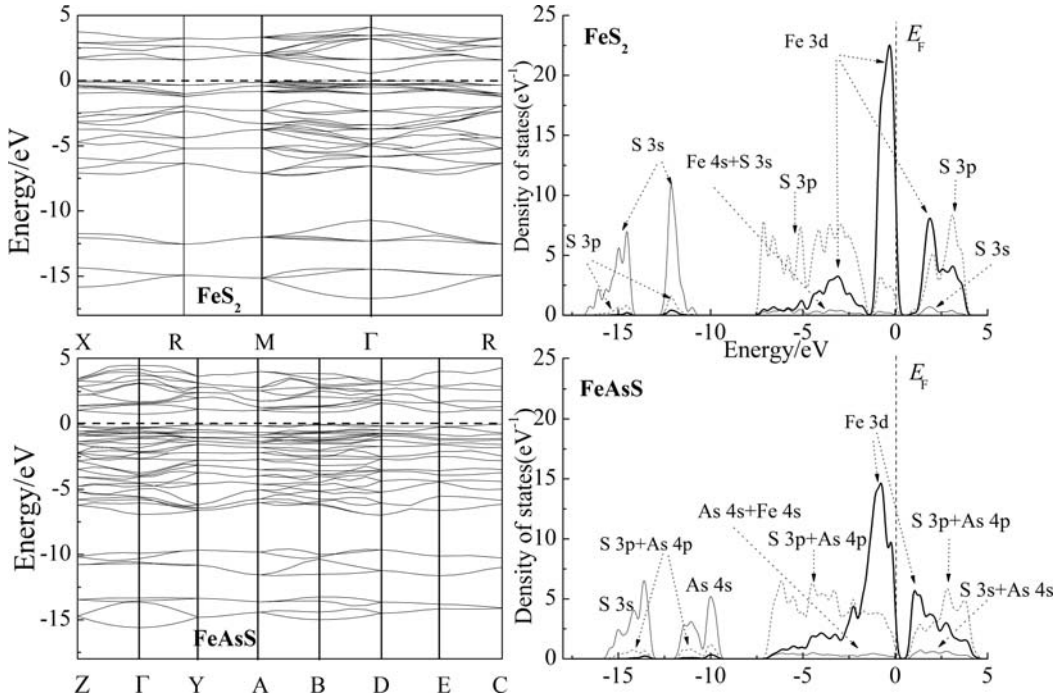


FIG. 3. Band structures and corresponding densities of states (DOS) of pyrite and arsenopyrite. The zero point of the energy has been set at the Fermi level, $E_F$.



https://doi.org/10.1180/minmag.2015.079.7.05 Published online by Cambridge University Press

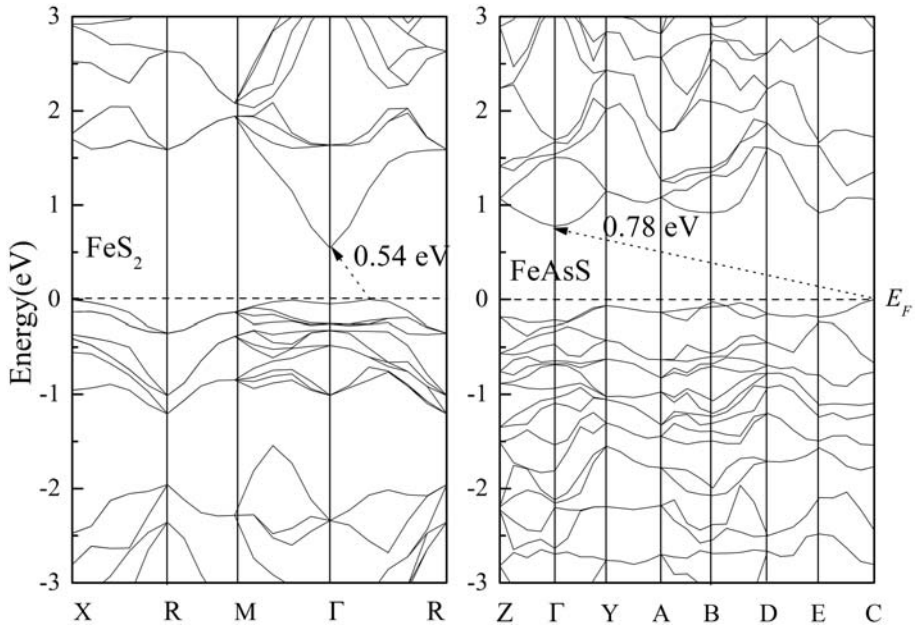


FIG. 4. Band structures of pyrite and arsenopyrite near the Fermi level. The dashed line depicts the Fermi level at the valence band maximum (VBM).

The electronic band structure of pyrite is split into five energy intervals between –17 and 5 eV. The two band groups between –17 and –10 eV have almost entirely S 3*s* character. The lower group of these two bands consists of the S–S bonding state, and the higher group consists of the S–S anti-bonding state. The band in the range from –7.5 to –1.5 eV, below the valence band maximum (VBM), is formed mainly from bonding Fe 3*d* and S 3*p* states. The band just below the Fermi level is formed from nonbonding S 3*p* and Fe 3*d* states. The conduction band is formed mainly from anti-bonding Fe 3*d* and S 3*p* states. These results are quite consistent with published studies (Edelro *et al*., 2003; Von Oertzen *et al*., 2005*a*,*b*; Womes *et al*., 1997; Opahle *et al*., 2000; Eyert *et al*., 1998). For arsenopyrite, there are four groups of bands in the energy range between –17 and 5 eV. The two groups between –17 and –10 eV are similar to those in pyrite. The lower group of these is derived mainly from As–S bonding states, and the higher group is formed from As–S anti-bonding states. The VBM is mainly derived from Fe 3*d*, As 4*p* and S 3*p* states with some contribution from As 4*s* and Fe 4*s* states. The conduction band is composed of S 3*p*, As 4*p* and Fe 3*d* states, with some contributions from S 3*s* and As 4*s* states.

Comparing the electronic structures of pyrite with arsenopyrite, it is clear that the pyrite valence band ranging from –7.5 to 0 eV is split at an energy of –1.25 eV, while this part of the valence band in arsenopyrite is continuous. Although the Fe 3*d* electrons are essentially localized in both pyrite and arsenopyrite, the pyrite Fe 3*d* orbital is split below the Fermi level, whereas the arsenopyrite Fe 3*d* orbital is not split, consistent with the Fe *L*-edge X-ray absorption near edge structure observation of arsenopyrite by Mikhlin and Tomashevich (2005), which demonstrated an almost unsplit 3*d*, e.g. singlet $Fe^{2+}$. This could be attributed to stronger Fe–S bonding atoms in pyrite than in arsenopyrite.

The electronic band structures of pyrite and arsenopyrite near the Fermi level are presented in Fig. 4. It shows that both pyrite and arsenopyrite are *p*-type semiconductors with indirect band gaps. The lowest points of the conduction bands for pyrite and arsenopyrite are located at the high symmetry Γ point. Calculated band gaps for pyrite and arsenopyrite are 0.54 and 0.78 eV, respectively. The calculated band gap of pyrite is smaller than the experimental value of 0.95 eV (Schlegel and Wachter, 1976) due to the *GGA-PW91* method, which commonly results in smaller gap values. Few reports on the optical band gap of arsenopyrite



https://doi.org/10.1180/minmag.2015.079.7.05 Published online by Cambridge University Press

could be found in the literature. Using the diffuse reflectance technique, Wood and Strens (1979) found that the band gap of arsenopyrite is less than 0.5 eV, slightly lower than our calculated result.

Interactions between the orbital electrons can be obtained by plotting the atomic DOS, as shown in Fig. 5. Figure 5*a* plots the *p-d* S–Fe interaction in pyrite. In the Fe octahedral ligand field, the 3*d* orbitals are split at the Fermi level into fully occupied non-bonding $t_{2g}$ states and empty anti-bonding $e_g^*$ states. The $t_{2g}$ state peak is sharp, and localization of the electrons is very strong. In addition, below the $t_{2g}$ states there exist non-local, bonding 3*d* $e_g$ states that are separated from the $t_{2g}$ states at –1.5 eV. These $e_g$ states interact with the S 3*p* states and form bonding states, while anti-bonding interactions occur between the $e_g^*$ state with the S 3*p* state in the conduction band.

The *p-d* Fe-S interaction in arsenopyrite is shown in Fig. 5*b*. The first distinct difference between the pyrite Fe–S atoms and the arsenopyrite Fe–S atoms is that the *d-p* orbitals of the latter do not split in the range of –7.5 to 0 eV, i.e. the bonding 3*d* $e_g$ states and the non-bonding 3*d* $t_{2g}$ states are connected. Another difference is that the bonding range between pyrite Fe–S atoms (–7.5 to –1.5 eV) is wider than that between arsenopyrite Fe–S atoms (–7.5 to –3 eV). However, the anti-bonding effect between pyrite Fe–S atoms is stronger than that between arsenopyrite Fe–S atoms, which causes the larger distance and weaker covalent bond between Fe–S in pyrite than in arsenopyrite. The As–S covalent interaction in arsenopyrite is also found to be greater than the S–S covalent interaction in pyrite. The *p-d* interaction between As–Fe atoms in arsenopyrite is shown in Fig. 5*c*. It is clearly shown that the bonding interaction between the As 4*p* and Fe 3*d* orbitals is very weak, while their anti-bonding effect is very strong, indicating anti-bonding interactions between the As and Fe

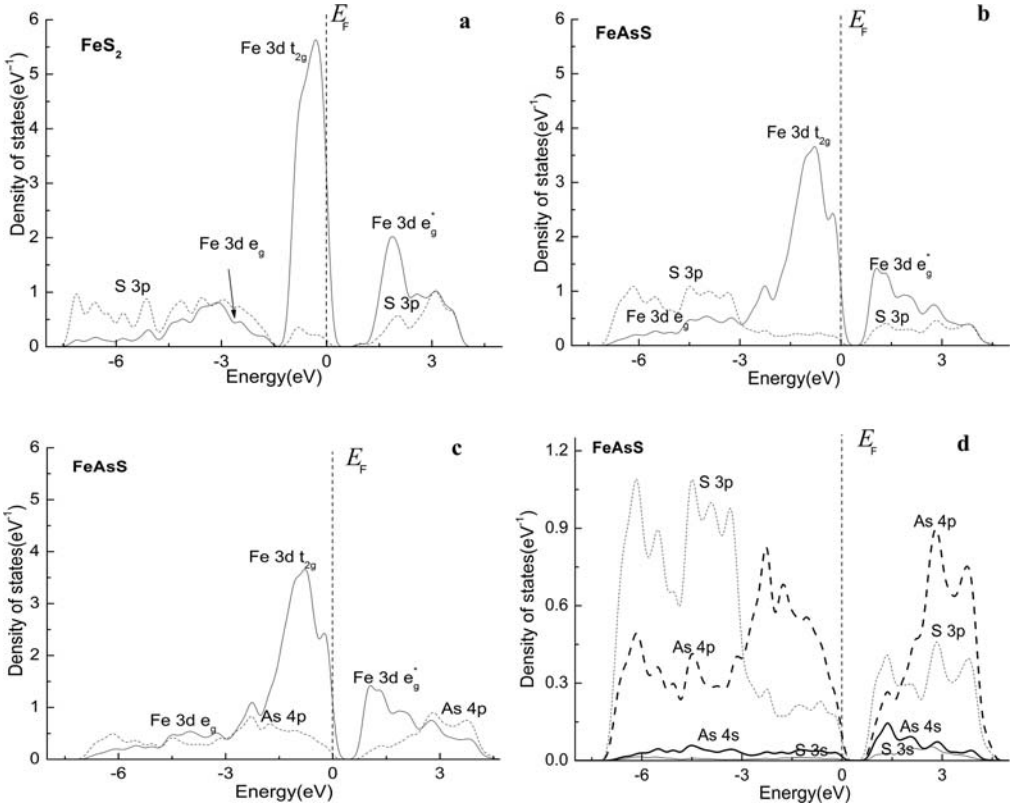


FIG. 5. DOS of (*a*) Fe and S atoms in pyrite; and (*b*) Fe and S atoms, (*c*) Fe and As atoms and (*d*) As and S atoms in arsenopyrite. The zero point of the energy has been set at the Fermi level, $E_F$.



https://doi.org/10.1180/minmag.2015.079.7.05 Published online by Cambridge University Press

TABLE 3. Fermi levels and orbital coefficients of pyrite and arsenopyrite.

| Mineral | Fermi level (eV) | Frontier orbital | Orbital coefficient |
|---|---|---|---|
| Pyrite | 5.99 | HOMO | 0.292Fe 3*d*, 0.035S 3*p* |
| | | LUMO | 0.009Fe 3*d*, 0.242S 3*p* |
| Arsennopyrite | 5.92 | HOMO | 0.323Fe 3*d*, 0.126S 3*p*, 0.264As 4*p* |
| | | LUMO | 0.401Fe 3*d*, 0.200S 3*p*, 0.090As 4*p* |

atoms, which is consistent with the calculated negative Mulliken population of the As–Fe bond. The orbital interactions between the As and S atoms in arsenopyrite are shown in Fig. 5*d*. The *p*-*p* orbital interaction occupies the predominant position during the As–S bonding process, and the *s* orbital electrons have little contribution to the interatomic bonding. The *p*-*p* bonding region is between –7.5 and –3 eV, and the anti-bonding region is located in the range of –3 to 0 eV.

### *Frontier orbit calculation*

The calculated Fermi levels ($E_F$) and orbital coefficients of pyrite and arsenopyrite are shown in Table 3. Statistical theory has proven that the Fermi level is the chemical potential of electrons in the system, expressed by equation 1,

$$E_F = \mu = \left(\frac{\partial G}{\partial N}\right)_T \quad (1)$$

where μ and $G$ are the chemical potential and free energy of the system, respectively, $N$ is the total number of electrons and $T$ is the temperature. According to the calculated Fermi levels of the minerals (Table 3), the $E_F$ values of pyrite (5.99 eV) and arsenopyrite (5.92 eV) are very close, which suggests that the electrochemical activities of these two minerals are very similar, resulting in difficult separation via simple electrochemical methods.

According to frontier molecular orbital (FMO) theory, interactions between molecules involve the highest occupied molecular orbital (HOMO) and the lowest unoccupied molecular orbital (LUMO). Moreover, regioselectivity is controlled by the orbital coefficients. A high value of the coefficient indicates a large contribution of the atom to the frontier orbital, while a low value indicates a small contribution. For pyrite, the Fe 3*d* orbital coefficient (0.292) in the highest occupied molecular orbital (HOMO) is far greater than that of S 3*p* (0.035), whereas the opposite situation occurs for the LUMO (0.009 for Fe 3*d* and 0.242 for S 3*p*). In the case of arsenopyrite, the Fe 3*d* orbital coefficient (0.323) in the HOMO is the largest, followed by the As 4*p* (0.265) and then the S 3*p* (0.124). For the LUMO, the Fe 3*d* orbital coefficient remains the largest, while the magnitude of the S 3*p* orbital coefficient is greater than that of the As 4*p*.

It is suggested that the LUMO of the $O_2$ molecule and the HOMO of the mineral will take part in interactions at the sulfide mineral surface. Based on the orbital coefficients for the HOMO, Fe atoms would be the most reactive sites for the interaction of pyrite with oxygen, while Fe, S and As (even more reactive than S) atoms all have potential as the reactive site for interactions of arsenopyrite and oxygen. Therefore, in addition to iron oxides and sulfate, oxidation products on arsenopyrite would include arsenate. In addition, it is apparent from the orbital coefficients that the oxidation of arsenopyrite by oxygen would be stronger than for pyrite. Studies by Corkhill *et al*. (2011) and Schaufuss *et al*. (2000) confirmed that As was more reactive than Fe in an oxidizing environment, and the reaction of oxygen with FeAsS surfaces revealed fast oxidation of As surface sites; therefore, As was likely to be the most favourable atom at the surface for the sorption of oxidizing species, such as $O_2$ and $H_2O$, thus promoting the production of As oxides and acids of As, such as $H_3AsO_3$ and $H_3AsO_4$. Based on these results, we conclude that the selective separation of arsenopyrite from pyrite may be possible using an oxidation mechanism. However, the oxidation process may be difficult to control.

In addition to oxidation, the interaction of a collector with a mineral surface is also very important for flotation. Generally, the interactions of collectors with sulfide minerals occur between the HOMO of the collector and the LUMO of the mineral, and the Fe atoms are the reactive sites. It is clear from the orbital coefficients of the LUMO that the activity of Fe in the pyrite LUMO is much



https://doi.org/10.1180/minmag.2015.079.7.05 Published online by Cambridge University Press

weaker than in the arsenopyrite LUMO, suggesting distinctive differences in the activity of Fe. Consequently, the separation of arsenopyrite and pyrite could be achieved by using the difference in chemical reactivities of iron in the two minerals. Iron does not often form stable compounds with amines; however, some complex amines species, such as EDTA, ethylenediamine and bipyridine, can form stable compounds with iron in aqueous solution. Using hexylthioethylamine as a collector, Sirkeci (2000) performed a flotation separation of pyrite from arsenopyrite. Using an unconventional anionic collector, sodium dodecylsulfonate, Kydros *et al*. (1993) performed the selective flotation of arsenopyrite from pyrite at pH ≈ 4 in a Hallimond cell from a bulk auriferous pyrite-arsenopyrite concentrate.

## Conclusions

Density functional calculations were performed on pyrite and arsenopyrite crystals to obtain their electronic and chemical structures. In arsenopyrite, Fe–Fe distances are alternately long and short with a short distance of 2.657 Å and a long distance of 3.746 Å. However, electron density calculations indicate that cation-cation interactions are very weak, and that cation-anion interactions are dominant in arsenopyrite. According to bond population calculations, the covalent character between Fe and S atoms in pyrite is weaker than in arsenopyrite. In addition, the covalent S–S interaction in pyrite is weaker than the As–S interaction in arsenopyrite. It is interesting that a strong anti-bonding interaction occurs between Fe and As atoms. The electronic structure results show that the pyrite Fe 3*d* orbitals below the Fermi level are very different to those in arsenopyrite. In addition, *d-p* orbital interactions between Fe and S atoms in pyrite are also very different from those in arsenopyrite. In arsenopyrite, the *p-p* orbital interaction is dominant for As–S bonding. From frontier orbital calculations, it is shown that, for pyrite, it is the Fe 3*d* electrons in the HOMO and the S 3*p* electrons in the LUMO that take part in reactions with other substances. In the case of arsenopyrite, in addition to Fe 3*d*, both the As 4*p* and S 3*p* electrons in the HOMO and LUMO would take part in reactions with other substances. It is apparent that the presence of As has a significant effect on the reactivity of arsenopyrite, and As atoms could be reactive sites for oxidation. According to the frontier orbital calculations, the separation of arsenopyrite and pyrite could be achieved by using the difference in chemical reactivities of iron in the minerals. Collector ions, which undergo strong chemical adsorption onto mineral surface Fe sites, could be used to achieve the flotation separation of arsenopyrite and pyrite.

## Acknowledgements

The authors are grateful for financial support provided by the National Natural Science Foundation of China (NSFC. 51304054 and NSFC. 51364002), the Ministry of education program for New Century Excellent Talents (NCET-11-0925) and the Guangxi Natural Science Foundation (2013GXNSFBA019259). They are also grateful for the support from the Shanghai Supercomputer Centre.

## References

Abraitis, P.K., Pattrick, R.A.D. and Vaughan, D.J. (2004) Variations in the compositional, textural and electrical properties of natural pyrite: a review. *International Journal of Mineral Processing*, **74**, 41–59.

Allison, S.A., Goold, L.A., Nicol, M.J. and Granville, A. (1972) A determination various solution, products of the products of reaction between sulfide minerals and aqueous xanthate and a correlation of the with electrode rest potentials. *Metallurgical Transactions*, **3**, 2613–2618.

Bayliss, P. (1977) Crystal structure refinement of a weakly anisotropic pyrite. *American Mineralogist*, **62**, 1168–1172.

Bayliss, P. (1989) Crystal chemistry and crystallography of some minerals within the pyrite group. *American Mineralogist*, **74**, 1168–1176.

Bindi, L., Moelo, Y., Leone, P. and Suchaud, M. (2012) Stoichiometric arsenopyrite, FeAsS, from La Roche-Balue Quarry, Loire-Atlantique, France: crystal structure and Mössbauer study. *The Canadian Mineralogist*, **50**, 471–479.

Blanchard, M., Alfredsson, M., Brodholt, J., Wright, K. and Catlow, C.R.A. (2007) Arsenic incorporation into $FeS_2$ pyrite and its influence on dissolution: a DFT study. *Geochimica et Cosmochimica Acta*, **71**, 624–630.

Buerger, M.J. (1936) The symmetry and crystal structure of the minerals of the arsenopyrite group. *Zeitschrift für Kristallographie*, **95**, 83–113.

Buerger, M.J. (1939) The crystal structure of gudmundite (FeSbS) and its bearing on the existence field of the arsenopyrite structural type. *Zeitschrift für Kristallographie*, **101**, 290–316.

Chanturiya, V.A., Fedorov, A.A. and Matveeva, T.N. (2000) The effect of auroferrous pyrites non-



https://doi.org/10.1180/minmag.2015.079.7.05 Published online by Cambridge University Press

stoichiometry on their flotation and sorption properties. *Physicochemical Problems of Mineral Processing*, **34**, 163–170.

Cocula, V., Starrost, F., Watson, S.C. and Carter, E.A. (2003) Spin-dependent pseudopotentials in the solid-state environment: applications to ferromagnetic and antiferromagnetic metals. *Journal of Chemical Physics*, **119**, 7659–7671.

Corkhill, C.L. Warren, M.C. and Vaughan, D.J. (2011) Investigation of the electronic and geometric structures of the (110) surfaces of arsenopyrite (FeAsS) and enargite ($Cu_3AsS_4$). *Mineralogical Magazine*, **75**, 45–63.

Edelro, R., Sandström, Å. and Paul, J. (2003) Full potential calculations on the electron bandstructures of sphalerite, pyrite and chalcopyrite. *Applied Surface Science*, **206**, 300–313.

Eyert, V., Höck, K.H., Fiechter, S. and Tributsch, H. (1998) Electronic structure of $FeS_2$: the crucial role of electron-lattice interaction. *Physical Review B*, **57**, 6350–6359.

Fernandez, P.G., Linge, H.G. and Wadsley, M.W. (1996) Oxidation of arsenopyrite (FeAsS) in acid. Part 1. Reactivity of arsenopyrite. *Journal of Applied Electrochemistry*, **26**, 575–583.

Finklea, S.L. Cathey, L. and Amma, E.L. (1976) Investigation of the bonding mechanism in pyrite using the Mössbauer effect and X-ray crystallography. *Acta Crystallographica*, **A32**, 529–537.

Fuess, H., Kratz, T., Topel-Schadt, J. and Miehe, G. (1987) Crystal structure refinement and electron microscopy of arsenopyrite. *Zeitschrift für Kristallographie*, **179**, 335–346.

Goodenough, J.B. (1960) Direct cation-anion interactions in several oxides. *Physical Review*, **117**, 1442–1551.

Goodenough, J.B. (1972) Energy bands in $TX_2$ compounds with pyrite, marcasite, and arsenopyrite structures. *Journal of Solid State Chemistry*, **5**, 144–152.

Hohenberg, P. and Kohn, W. (1964) Inhomogeneous electron gas. *Physical Review B*, **136**, 864–871.

Huggins, M.L. (1922) The crystal structures of marcasite ($FeS_2$), arsenopyrite (FeAsS) and loellingite ($FeAs_2$). *Physical Review*, **19**, 369–373.

Hulliger, F. and Mooser, E. (1965) Semiconductivity in pyrite, marcasite and arsenopyrite phases. *Journal of Physics and Chemistry of Solids*, **26**, 429–433.

Kohn, W. and Sham, L.J. (1965) Self-consistent equations including exchange and correlation effects. *Physical Review*, **140**, A1133–A1138.

Kydros, K.A., Matis, K.A., Papadoyannis, I.N. and Mavros, P. (1993) Selective separation of arsenopyrite from an auriferous pyrite concentrate by sulphonate flotation. *International Journal of Mineral Processing*, **38**, 141–151.

Mikhlin, Y. and Tomashevich, Y. (2005) Pristine and reacted surfaces of pyrrhotite and arsenopyrite as studied by X-ray absorption near-edge structure spectroscopy. *Physics and Chemistry of Minerals*, **32**, 19–27.

Monkhorst, H.J. and Pack, J.D. (1976) Special points for Brillouin-zone integrations. *Physical Review B*, **13**, 5188–5192.

Morimoto, N. and Clark, L.A. (1961) Arsenopyrite crystal-chemical relations. *American Mineralogist*, **46**, 1448–1469.

Nickel, E.H. (1968) Structural stability of minerals with the pyrite, marcasite, arsenopyrite and loellingite structures. *The Canadian Mineralogist*, **9**, 311–321.

Opahle, I., Koepernik, K. and Eschrig, H. (2000) Full potential band structure calculation of iron pyrite. *Computational Materials Science*, **17**, 206–210.

Pack, J.D. and Monkhorst, H.J. (1977) "Special points for Brillouin-zone integrations"-a reply. *Physical Review B*, **16**, 1748–1749.

Perdew, J.P., Chevary, J.A., Vosko, S.H., Jachson, K.A., Pederson, M.R., Singh, D.J. and Fiolhais, C. (1992) Atoms, molecules, solids, and surfaces: applications of the generalized gradient approximation for exchange and correlation. *Physical Review B*, **46**, 6671–6687.

Prince, K.C., Matteucci, M., Kuepper, K., Chiuzbaian, S. G., Barkowski, S. and Neumann, M. (2005) Core-level spectroscopic study of FeO and $FeS_2$. *Physical Review B*, **71**, 085102-1–085102-9.

Ramsdell, L.S. (1925) The crystal structure of some metallic sulfides. *American Mineralogist*, **10**, 281–304.

Schaufuss, A.G., Nesbitt, H.W., Scaini, M.J., Hoechst, H., Bancroft, M.G. and Szargan, R. (2000) Reactivity of surface sites on fractured arsenopyrite (FeAsS) toward oxygen. *American Mineralogist*, **85**, 1754–1766.

Schlegel, P. and Wachter, P. (1976) Optical properties, phonons and electronic structure of iron pyrite (FeS). *Journal of Physics C: Solid State Physics*, **9**, 3363–3369.

Segall, M.D., Shah, R., Pickardk, C.J. and Payne, M.C. (1996) Population analysis of plane-wave electronic structure calculations of bulk materials. *Physical Review B*, **54**, 16317–16320.

Sirkeci, A.A. (2000) The flotation separation of pyrite from arsenopyrite using hexyl thioethylamine as collector. *International Journal of Mineral Processing*, **60**, 263–276.

Tossell, J.A., Vaughan, D.J. and Burdett, J.K. (1981) Pyrite, marcasite, and arsenopyrite type minerals: crystal chemical and structural principles. *Physics and Chemistry of Minerals*, **7**, 177–184.

Vanderbilt, D. (1990) Soft self-consistent pseudopotentials in a generalized eigenvalue formalism. *Physical Review B*, **41**, 7892–7895.

Von Barth, U. and Hedin, L.A. (1972) Local exchange-correlation potential for the spin polarized case. *Journal of Physics C*, **5**, 1629–1642.



https://doi.org/10.1180/minmag.2015.079.7.05 Published online by Cambridge University Press

Von Oertzen, G.U., Jones, R.T. and Gerson, A.R. (2005*a*) Electronic and optical propenies of Fe, Zn and Pb sulfides. *Physics and Chemistry of Minerals*, **32**, 255–268.

Von Oertzen, G.U., Skinner, W.M. and Nesbitt, H.W. (2005*b*) Ab initio and X-ray photoemission spectroscopy study of the bulk and surface electronic structure of pyrite (100) with implications for reactivity. *Physical Review B*, **72**, 235427-1–235427-10.

Vosko, S.J., Wilk, L. and Nusair, M. (1980) Accurate spin-dependent electron liquid correlation energies for local spin density calculations: a critical analysis. *Canadian Journal of Physics*, **58**, 1200–1211.

Womes, M., Karnatak, R.C., Esteva, J.M., Lefebvre, I., Alla, G. Olivier-Fourcade, J. and Jumas, J.C. (1997) Electronic Structures of FeS and $FeS_2$: X-ray absorption spectroscopy and band structure calculations. *Journal of Physical Chemistry Solids*, **58**, 345–352.

Wood, B.J. and Strens, R.G.J. (1979) Diffuse reflectance spectra and optical properties of some sulphides and related minerals. *Mineralogical Magazine*, **43**, 509–518.



https://doi.org/10.1180/minmag.2015.079.7.05 Published online by Cambridge University Press